Clean Techn Environ Policy (2007) 9:289–311
DOI 10.1007/s10098-006-0083-2

ORIGINAL PAPER

Conceptual design of carbon nanotube processes

Adedeji E. Agboola · Ralph W. Pike · T. A. Hertwig · Helen H. Lou

Received: 9 October 2006 / Accepted: 22 November 2006 / Published online: 10 January 2007

Abstract Carbon nanotubes, discovered in 1991, are a new form of pure carbon that is perfectly straight tubules with diameter in nanometers, length in microns. The conceptual designs of two processes are described for the industrial-scale production of carbon nanotubes that are based on available laboratory synthesis techniques and purification methods. Two laboratory-scale catalytic chemical vapor deposition reactors were selected for the conceptual design. One (CNT-PFR process) used the high-pressure carbon monoxide disproportionation reaction over iron catalytic particle clusters (HiPCO reactor), and the other (CNT-FBR process) used catalytic disproportionation of carbon monoxide over a silica supported cobalt–molybdenum catalyst (CoMoCAT reactor). Purification of the carbon nanotube product used a multi-step approach: oxidation, acid treatment, filtration and drying. Profitability analysis showed that both process designs were economically feasible. For the CNT-PFR process, the net present value, based on a minimum attractive rate of return of 25% and an economic life of 10 years, was $609 million, the rate of return was 37.4% and the economic price was $38 per kg of carbon nanotube. For the CNT-FBR process, the net present value was $753 million, rate of return was 48.2% and the economic price was $25 per kg of carbon nanotube. The economic price for these processes is an order of magnitude less than the prevalent market price of carbon nanotubes and is comparable to the price of carbon fibers.

Keywords Carbon nanotubes · Conceptual design · Carbon monoxide disproportionation reaction · Cobalt–molybdenum catalyst · Iron pentacarbonyl catalyst · Profitability analysis · Purification methods for carbon nanotubes

A. E. Agboola · R. W. Pike (✉)
Louisiana State University, Baton Rouge 70803, USA
e-mail: pike@lsu.edu

T. A. Hertwig
Mosaic Inc., Uncle Sam, LA, USA

H. H. Lou
Lamar University, Beaumont, TX, USA

Introduction

Carbon nanotubes are a new form of pure carbon that is perfectly straight tubules with diameter in nanometers, length in microns and properties close to those of an ideal graphite fiber (Ajayan 2000). Discovered in 1991, carbon nanotubes have caught the attention of scientists, engineers and investors because of their remarkable mechanical and electronic properties: 100 times the tensile strength of steel, thermal conductivity better than all but the purest diamond, and electrical conductivity similar to copper. The biggest challenge in developing potential applications for carbon nanotubes is the production of pure carbon nanotubes in commercial quantities at affordable prices.

A molecular model of the armchair configuration (others are zigzag and chiral) is shown in Fig. 1. A typical laboratory apparatus is shown in Fig. 2, and a mixture of configurations of carbon nanotubes is produced. Photographs of carbon nanotubes are shown in Fig. 2, also.

Current synthesis methods have limited production capacity, and the market price is around $200/g for

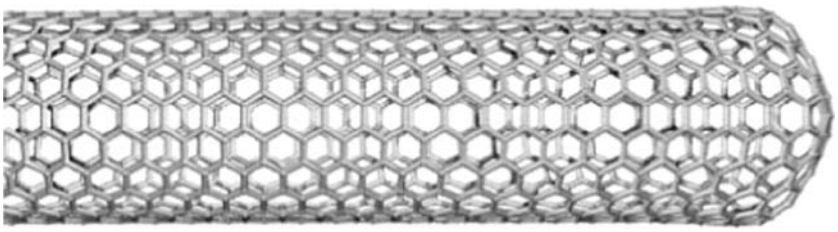

Fig. 1 Molecular model of a single-walled carbon nantube, from Terrones (2003)

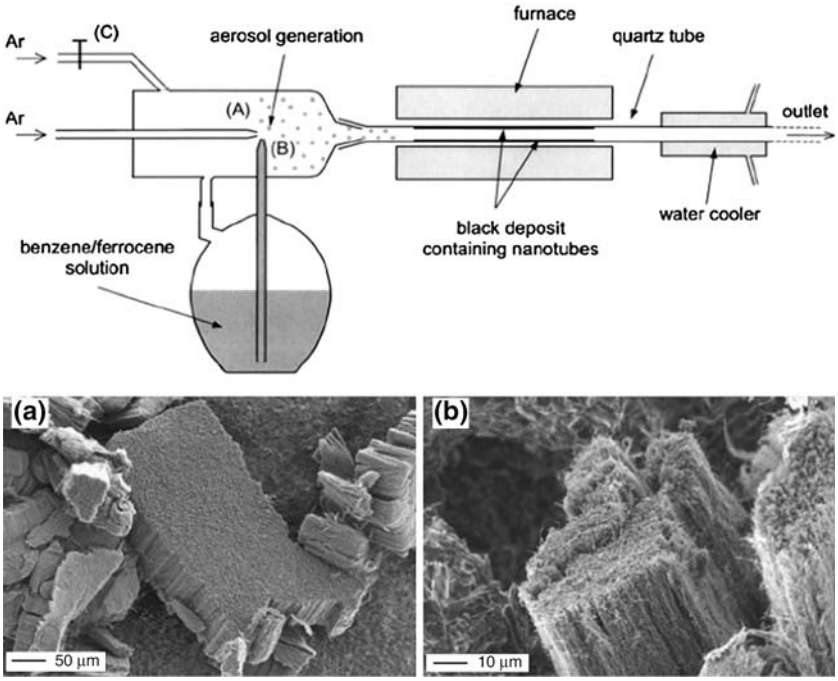

Fig. 2 Laboratory apparatus for production of carbon nanotubes

multi-wall carbon nanotubes (MWNT) to ten times this value for purified single-wall carbon nanotubes (SWNT). A laboratory apparatus and carbon nanotubes produced it are shown in Fig. 2. There are forty-four global producers of carbon nanotubes with a current global production of single-walled carbon nanotubes estimated to be about 9,000 kg/year. Presently, almost one-half of the multi-walled carbon nanotube production takes place in the United States, followed by Japan with ~40% of total production. Likewise, the United States leads production of single-wall carbon nanotubes with more than 70% total production capacity (Agboola 2005). The development of large-scale commercial production of carbon nanotubes at accessible costs is essential to emerging and potential carbon nanotube technologies.

In recent years, the interest in carbon nanotube has overshadowed that of fullerenes. Carbon nanotubes are not as readily available as fullerenes, and the number of researchers and groups working in the nanotube field has increased significantly. This has led to an exponential growth in the number of nanotube publications, going from 100 in 1994 to 1,500 in 2001 (Terrones 2003).

A review of the synthesis techniques, growth mechanism, and purification methods for carbon nanotubes is given next. This information is used to for the conceptual design of industrial-scale processes for carbon nanotubes.

Carbon nanotube synthesis methods

An extensive literature review of the laboratory-scale synthesis techniques for carbon nanotube has been reported by Agboola (2005). The review includes reactor design, energy requirements, temperature, pressure, voltage, current, coolant flow rate, graphite evaporation rate and electrode diameter. It also includes reactants, products, catalysts, carrier gas, conversion, carbon nanotube yield and selectivity as well as the purification techniques. A summary is given

with tables describing key laboratory-scale reactors and purification methods to produce single and multi-wall carbon nanotubes.

Synthesis methods

The three main methods of producing carbon nanotubes are electric arc discharge, laser vaporization, and chemical vapor deposition and are described below. Other techniques include electrolytic synthesis, and a solar production method, among others and are reviewed by Agboola (2005).

Arc discharge

In this method carbon nanotubes are produced from the carbon vapor generated by an arc discharge between two graphite electrodes (with or without catalysts), under an inert gas atmosphere. Typical synthesis conditions for the carbon arc discharge method employ a direct current of 50–100 A and a voltage of 20–25 V operating in an inert atmosphere. The magnitude of the current required is proportional to the diameter of the electrode, as higher currents are needed to vaporize larger electrodes (Dresselhaus et al. 1996).

Typical of the methods and results using electric arc discharge were given by Lee et al. (2002), who described the synthesis of carbon nanotubes by plasma rotating arc discharge. Carbon nanotubes were formed by the condensation of high-density carbon vapor transferred out of the plasma region by the centrifugal force generated by the rotation of the electrodes. The rotating electrode prevented the local concentration of the electric field, and spread the micro-discharge uniformly over the whole electrodes, thus ensuring a higher discharge volume and more stable plasma. As the rotating speed of the electrode increased (0–10,000 rev/min), the plasma volume increased and the collector temperature rose. The supply of the carbon vapor and the temperature of the collector determined the nanotube growth, and the nanotube yield increased as the rotation speed of the anode increased. Reactor pressure was 500 Torr, discharge current of 80–120 A with voltage ~20–30 V using pure graphite electrodes, anode 12 mm OD and cathode 15 mm OD, helium carrier gas and a ~80% yield. Purification was by heating at 700 C in air. Journet et al. (1997) reported a similar procedure except that their carbon nanotubes were produced by an arc discharge between two electrodes, a graphite cathode and a graphite anode, in which a hole had been drilled and filled with a mixture of metallic catalyst (Ni–Co, Co–Y, or Ni–Y) and graphite powders. The reaction products consisted of large amount of entangled carbon filaments, homogeneously distributed over large areas with diameters ranging from 10 to 20 nm. Each carbon filament consisted of smaller aligned SWNTs; self organized into bundle-like crystallites with diameters ranging from 5–20 nm. The carbon nanotube yield (with respect to the total volume of the solid material) was estimated to be of the order of 80%.

Laser vaporization

In 1995, Smalley and co-workers (Guo et al. 1995), at Rice University found a relatively efficient method to synthesize single walled carbon nanotubes using laser vaporization of a carbon target. The laser vaporization technique involved the use of a pulsed or continuous laser to vaporize a graphite target, containing a small amount of transition metal particle catalysts, inside a tube furnace heated to 1,200 C in an inert gas atmosphere. The laser vaporized the metal–graphite target and nucleated carbon nanotubes in the shockwave just in front of the target, while flowing argon gas swept the vapor and nucleated nanotubes, which continued to grow, from the furnace to a water-cooled copper collector (Meyyappan and Srivasta 2003). Multi-walled carbon nanotubes were generated by this method when the vaporized carbon target was pure graphite whereas the addition of transition metals (Co, Ni, Fe or Y) as catalysts to the graphite target resulted in the production of single walled carbon nanotubes. The single-walled carbon nanotubes formed, existed as 'ropes' and were bundled together by van der Waals forces (Dresselhaus et al. 1996).

Typical methods and results for laser vaporization were given by Guo et al. (1995). Single-wall carbon nanotubes were synthesized from a mixture of carbon and transition metals by a laser impinging on a transition metal–graphite composite target. In contrast to the arc technique, direct vaporization allowed far greater control over growth conditions, permitted continuous operation, and produced better quality nanotubes in higher yield. A series of mono- and bi-metal catalysts were evaluated for yield and quality of single walled carbon nanotubes: Ni, Co, Cu, Nb, Pt, Co/Ni, Co/Pt, Co/Cu, Ni/Pt. For mono-catalysts, Ni produced the highest yield, while Co/Ni and Co/Pt bi-metal catalysts yielded SWNTs in high abundance with yields 10–100 times the single metals alone. The carbon nanotube yields were observed to increase with temperature up to the furnace limit of 1,200 C. The reactor was a quartz tube mounted in high temperature furnace and operated at 1,200 C and 500 Torr. The laser source was a Continuum DCR-16S 300 mJ/pulse

at 0.532 μm in an atmosphere of argon. Yields were 15–50% and purification was by sonication in methanol.

Chemical vapor deposition

This technique involved the use of an energy source, such as a plasma, a resistive or inductive heater, or furnace to transfer energy to a gas-phase carbon molecule over metal catalysts deposited on substrates to produce fullerenes, carbon nanotubes and other sp^2-like nanostructures (Meyyappan 2004). Commonly used gaseous carbon sources included carbon monoxide and hydrocarbon feedstock such as methane, acetylene, ethylene, and *n*-hexane.

The chemical vapor deposition (CVD) technique can be applied both in the absence and presence of a substrate; the former being a gas-phase homogeneous process where the catalyst is in the gas-phase, the latter being a heterogeneous process using a supported catalyst (Corrias et al. 2003). The CVD technique can be used to preferentially synthesize single or multi-walled nanotubes depending on the choice of appropriate metal catalyst.

Carbon nanotubes generated by the template-based chemical vapor deposition technique exhibit excellent alignment and positional control on a nanometer scale. The size of the particles and pores, which determine the size of the nanotubes, can be controlled prior to carbon deposition. By regulating the amount of carbon feedstock supplied and the thickness of the membranes, the length of the carbon nanotubes formed can be controlled (Ajayan 2000).

Chemical vapor deposition synthesis techniques can be categorized according to the energy source: thermal chemical vapor deposition and plasma enhanced chemical vapor deposition (PECVD). Thermal chemical vapor deposition uses conventional heat source as its energy source, while a plasma source is used to create a glow discharge in the plasma enhanced chemical vapor deposition (PECVD).

A typical thermal CVD growth run involves purging the reactor with argon or some other inert gas in order to prevent the oxidation of the nano-size fine catalytic particles while increasing the reactor temperature to the desired growth temperature (Han and Yoo 2002). The undiluted reaction gas, which is either carbon monoxide or some hydrocarbon, is metered through a mass flow controller and fed through one end of the apparatus while the gas outlet is at the other end. At the end of the reaction period, the flow is switched back to the inert gas while the reactor cools down to prevent damage to the carbon nanotube produced due to exposure to air at elevated temperatures (Meyyappan 2004).

Carbon nanotubes produced by thermal chemical vapor deposition use either a plug flow reactor or a solid catalyst in a fixed or fluidized bed reactor and carbon monoxide is the reactant. Bronikowski et al. (2001), described a plug flow reactor (a high-pressure quartz tube reactor in a tube furnace) for the production of single wall carbon nanotubes from carbon monoxide disproportionation (decomposition into C and CO_2) over iron catalysts at high-pressure (30–50 atm), and high-temperature (900–1,100 C) that was called the HiPCO process. The iron catalytic clusters, formed in situ from the decomposition of the catalyst precursor, iron pentacarbonyl, acted as nuclei upon which the carbon nanotubes nucleate and grow. The effect of process parameters such as temperature, carbon monoxide pressure, and catalyst concentration on the growth rate of carbon nanotubes were investigated. Carbon nanotubes of up to 97% purity, at production rates of up to 450 mg/h have been reported for a carbon monoxide flow rate of 9.8l l/min. The process employed a closed loop through which unconverted carbon monoxide was continuously recycled.

Carbon nanotube formation by the carbon monoxide disproportionation (decomposition into C and CO_2) over iron catalysts at high-pressure (30–50 atm), and high-temperature (900–1,100 C) occurs via carbon monoxide disproportionation over iron particles according to the Boudouard mechanism (equation is not balanced)

$$CO_{(g)} + CO_{(g)} \rightarrow CO_{2(g)} + C_{(CNT)}. \quad (1)\leftarrow$$

Although, the detailed reaction mechanism and rate data for the catalyzed Boudouard reaction is not available, it can be inferred that the rate of the gas-phase reaction scales as a square of the carbon monoxide reactant gas partial pressure. The use of high-pressure carbon monoxide is essential for efficient carbon nanotube production, and hence, the use of a high-pressure (30–50 bar) flow reactor in the HiPCO reactor.

Resasco et al. (2001), described the development of a catalytic method (CoMoCAT process) that synthesized high quality single-walled carbon nanotubes (SWNTs) at very high selectivity and with a remarkably narrow distribution of tube diameter. In this technique, SWNTs were produced by CO disproportionation at 700–950 C and 1.0–10 atm pressure with a flow of pure CO. A production rate of ~0.25 g SWNT/g catalyst with a selectivity of ≥80% was reported. The synergistic effect between Co and Mo catalysts was

essential in its performance, such that the catalyst was only effective when both metals were simultaneously present on a silica support with low Co:Mo. Separated, they were either inactive (Mo alone) or unselective (Co alone). The SWNT produced were characterized by TEM, SEM, AFM, Raman spectroscopy and temperature programmed oxidation (TPO). For purification, treatment with 2 M NaOH solution was used to remove SiO_2, Mo and Co, and oxidation in air at 200–250 C and acid (HCl/HNO_3) was used to remove amorphous carbon.

The plasma enhanced CVD (PECVD) synthesis technique combines non-equilibrium plasma reaction, such as hot filament plasma, microwave plasma, radio frequency plasma and D.C. glow plasma, with template-controlled growth technology to synthesize carbon nanotubes at low process temperature (Li et al. 2004). The plasma reactor consists of a pair of electrodes in a chamber or reaction furnace, with one electrode grounded and the second connected to a high frequency power supply. The hot filament directly heats the catalytic substrate, placed on the grounded electrode, while the carbon rich feedstock such as ethylene, methane, ethane, and carbon monoxide is supplied from the opposite plate to the reaction chamber during the discharge. Carbon nanotubes grow on the nano-size fine metal particles, formed on the catalytic substrate, by the glow discharge generated from the high frequency discharge. The PECVD technique requires relatively low gas pressure and complex vacuum equipments (Li et al. 2004). The relatively low process temperature of PECVD is useful in semiconductor device fabrication (Meyyappan 2004).

Other investigators reporting the synthesis of carbon nanotubes by CVD include Mauron et al. (2003) who used iso-pentane (C_5H_{12}) on a magnesium oxide (MgO) powder impregnated with an iron nitrate ($Fe(NO_3)_3{\cdot}9H_2O$) in a fluidized-bed reactor operated at 450–800 C with a synthesis time of 0.5–40 min and produced MWNT while SWNT (700–800 C) were synthesized with acetylene. Purification included using HCl at 75 C to remove MgO. Liu et al. (2002) described the synthesis of MWNT using a tubular quartz reactor placed in a furnace at 800–1,000 C at atmospheric pressure using toluene and ferrocene as catalyst precursor. The pyrolysis temperature, ferrocene concentration, solution feeding rate and carrier gas flow rate all influenced the yield of carbon nanotubes. A carbon nanotube yield of 32 wt% was observed at a flow rate of 0.1 ml/min, using 10 wt% ferrocene/toluene solution and a hydrogen/argon carrier gas flow rate of 150 ml/min at a pyrolysis temperature of 900 C. Lyu et al. (2004) conducted similar experiments with Fe–Mo/MgO catalyst ethylene at 800 C, and Andrews et al. (2002), produced MWNT with xylene and ferrocene at temperatures in the range 625–775 C in a quartz tube in a multi-zone furnace. Details of numerous other similar experiments are given by Agboola (2005).

Growth mechanism

Carbon is the only elemental material that forms hollow tubes, perhaps as a result of the strong surface energy anisotropy of graphite basal planes compared to other lattice planes (Iijimaet al. 1992). As shown in Figs. 1 and 2 carbon nanotubes consist of concentric cylinders of hollow carbon hexagonal networks arranged around one another, often with a helical twist with the tips of the tubes almost always closed, with the presence of pentagons in the hexagonal lattice (Iijima et al. 1992).

The actual mechanism which carbon forms nanotubes is not understood, and various growth models based on experimental and quantitative studies have been proposed. It seems likely that two different mechanisms operate during the growth of MWNTs and SWNTs, because the presence of a catalyst is absolutely necessary for the growth of the latter (Ajayan 2000).

One school of thought assumes that the tubes are always capped and that the growth process involves a C_2 absorption process that is aided by the pentagonal defects on the cap. The second school of thought assumes the tubes are open during the growth process and that carbon atoms are added at the open ends of the tubes (Dresselhaus et al. 1996).

Evaluation of synthesis methods

The extensive literature review reported by Agboola (2005) was used to determine reactor type and dimensions, energy requirements, operating conditions including process temperatures and pressures. This review included the reactants products, catalysts, conversion, carbon nanotube yield and selectivity as well as purification techniques employed in experimental studies. Results describing key laboratory-scale production and purification methods were summarized for each of the methods to produce single and multi-wall carbon nanotubes. Detailed tables were prepared by Agboola (2005) that compared synthesis methods giving carbon source, catalyst, reactor operating conditions (arc-discharge, laser vaporization, and chemical vapor deposition), temperature, pressure, conversion and yield. Using this information, criteria for conceptual

designs included capital and operating cost, raw materials selection, operation mode (semi-batch, batch or continuous), production and purification methods. The process operating conditions, such as pressure, temperature, catalyst performance, reactant conversion and selectivity, were considered. The process conditions, such as operating temperature and pressure were important criteria for the conceptual designs because a lower operating temperature and pressure have lower operating costs and energy requirements. Catalyst performance, which includes its activity, deactivation time, and regeneration method, determined the extent of reaction, as well as the process selectivity to the desired product.

Generally, the carbon nanotubes synthesized by the high-temperature electric arc or laser vaporization processes have fewer structural defects, in addition to superior mechanical and electrical properties, than the low-temperature chemical vapor deposition processes. Electric arc and laser ablation processes are limited due to their elaborate configurations. It appears that the economical reasonable limit for the arc process has been reached at a production rate of ~100 g/h of raw carbon nanotubes (Moravsky et al. 2005).

Catalytic chemical vapor deposition operates at a lower temperature and is technically simpler than the arc or laser ablation. It is considered to be an economical route for the tons/day production of carbon nanotubes. Catalytic chemical vapor deposition has a higher selectivity to form carbon nanotubes than arc and laser vaporization, and the electric-arc discharge and laser vaporization methods result in mixtures of carbon materials (Perez-Cabero et al. 2003).

An analysis of the chemical vapor deposition production processes was based on criteria such as process operating conditions, selectivity, continuous growth, and yield. The conclusion was that the high-pressure carbon monoxide disproportionation (HiPCO) reactor and the cobalt–molybdenum fluidized bed catalytic (CoMoCAT) reactor were the two better choices for the conceptual design.

The high-pressure carbon monoxide (HiPCO) reactor has catalytic particles formed in situ by thermal decomposition of iron carbonyl. The process can be operated continuously by using continuous filtration to separate the carbon nanotubes containing the iron catalyst from the unreacted carbon monoxide. Carbon nanotubes contain iron particles (~5–6 at.%) that are formed from the decomposition of the iron carbonyl which act as the growth nucleation sites. The iron nanoparticles are not enclosed in heavy graphitic shells as in the arc or laser vaporization processes and are relatively easier to remove. A major drawback of the HiPCO reactor is the low rate of carbon monoxide conversion (~15–20% per cycle) even at high pressure. The unconverted carbon monoxide feedstock can be recycled to the reactor (Bronikowski et al. 2001). A commercial process using the HiPCO reactor is being developed by Carbon Nanotechnologies Incorporation, Houston, TX, a start-up company from Rice University.

The cobalt–molybdenum fluidized bed catalytic (CoMoCAT) reactor employs the synergistic effect between the cobalt and molybdenum to give high selectivity (better than 80%) to carbon nanotubes from CO disproportionation at 700–950 C and a total pressure ranging from 1 to 10 atm. Carbon monoxide disproportionation reaction is exothermic and can be limited by equilibrium at the high temperatures required to activate CO on the catalyst. High carbon monoxide pressures are used in order to mitigate the temperature effect and enhance the formation of carbon nanotubes. Resasco et al. (2001), reported that the extent of Co–Mo interaction is a function of the Co:Mo ratio in the catalyst. At low Co:Mo ratios, Co interacts with Mo in a superficial cobalt molybdate-like structure, whereas at high ratios, it forms a non-interacting Co_3O_4 state. The formation of carbon nanotubes is enhanced at low Co:Mo ratios because the Co:Mo interaction inhibits the cobalt sintering that usually results at the high temperatures.

The CoMoCAT fluidized bed reactor would give intimate contact between CO and the silica supported Co–Mo catalyst powder with high specific surface area. The residence times of the carbon nanotube could be controlled, and the activity of the catalyst utilized to ensure high conversion. There would be efficient heat and mass transfer between the carbon nanotube agglomerates and the bulk gas phase to have temperature control as needed to more-closely approach equilibrium. The carbon nanotubes formed in the CoMoCAT reactor are attached to the silica-supported catalyst particles, and an effective sequence of purification processes is required to remove these impurities. A commercial process using the CoMoCAT reactor is being developed by SouthWest Nanotechnologies, Inc., Norman, OK, a start-up company from the University of Oklahoma.

Purification methods

The carbon nanotubes, as produced by the various synthesis techniques, contain impurities such as graphite nanoparticles, amorphous carbon, smaller fullerenes, and metal catalyst particles. These impurities have to be separated from the carbon nanotubes before they can be

used for applications such as composites, nanoelectronics, etc. Purification techniques have been devised in other to improve the quality and yield of carbon nanotubes, and these methods include oxidation, acid treatment, annealing, micro filtration, ultrasonication, ferromagnetic separation, functionalization and chromatography techniques. A detailed literature review of these purification processes is given by Agboola (2005), and important details about these methods are summarized in the following paragraphs.

Oxidation

Amorphous carbon is oxidized more readily than carbon nanotubes, and the first technique devised to purify carbon nanotubes relied on the oxidation behavior of carbon nanotubes at temperatures greater than 700 C in air or in pure oxygen. The main shortcoming of the oxidative treatment is the high likelihood of the carbon nanotubes being oxidized during impurities oxidation. Carbon nanotube yield from the oxidative treatment in air/oxygen is usually poor. Carbon nanotube reactivity, measured using thermo gravimetric analysis, showed that the onset of carbon nanotube weight loss begins at about 700 C, with significant decrease in mass thereafter. Carbon nanotubes are oxidized completely to carbon monoxide and carbon dioxide at about 860 C (Terrones 2003).

The oxidative treatment of carbon nanotubes in air/oxygen removes carbonaceous impurities such as amorphous carbon and helps expose the catalytic metal surface enclosed in the carbon nanotube for further purification techniques. For example, Park et al. (2001) used an annealing apparatus consisting of two quartz tubes where the inner tube containing the MWNTs, was rotated inside the outer tube at the rate of 30 rpm at 760 C in ambient air. The quality and yield of the carbon nanotubes obtained was determined by the annealing time, and yield as high as 40% were reported.

Acid treatment

Acid treatment of single wall carbon nanotubes is used to remove metal catalyst from the reaction products. The treatment is usually preceded by a mild oxidation or sonication step to clear and expose the metal surface followed by the solvation of the metal catalyst on exposure to an acid while the carbon nanotubes remain in suspended form. Chiang et al. (2001a), reported using nitric acid to remove catalytic metals from laser-ablation grown single-walled carbon nanotubes. Then methanol wash was used followed by oxidation with 5% O_2/Ar at 1.0 atm at 300 and 500 C. Then extraction was performed with concentrated HCl solution to remove catalytic metals (Co and Ni) followed by drying in a vacuum at 150 C. The final metal content after the second gas-phase oxidation at 500 C was about 0.1 atomic percent relative to carbon, and carbon nanotube purity 99.9% was reported.

Chiang et al. (2001b), reported a method for extracting iron metal catalyst and amorphous carbon from single-wall carbon nanotubes produced in the HiPCO reactor. It involved low temperature, metal catalyzed, wet air oxidation of nanotubes to selectively remove amorphous carbon and enable extraction of iron with concentrated HCl. Filtering with water/methanol and annealing at 800 C gave carbon nanotubes with a catalytic metal content of less than 1.0% (wt).

Other investigators have reported similar results using mineral acids to remove metal catalysts and oxidation to remove amorphous carbon. Hou et al. (2002), described the benefit of ultrasonication. Carbon nanotubes with purity greater than 94% were obtained, and yields of the purified material varied from 30 to 50%, depending on the oxidation time and temperature. Harutyunyan et al. (2002), used microwave heating followed by a mild acid treatment to remove most of the catalytic metals in the sample, and the purified single-walled carbon nanotubes reportedly contained a residual metal level lower than 0.2 wt%. Details of numerous other similar experiments are given by Agboola (2005).

Ultrasonication

This purification technique involves the separation of particles using ultrasonic vibrations which agglomerates different nanoparticles undergoing forced vibration, and they become more dispersed. The separation efficiency is dependent on the surfactant, solvent and reagents used.

Shelimov et al. (1998), reported using an ultrasonically-assisted filtration method for the purification of single wall carbon nanotubes produced by the laser-vaporization process. Ultrasonication applied to the sample during filtration maintained the material in suspension and prevented cake formation on the surface of the filter. The as-produced SWNT soot, suspended in toluene, was filtered to extract soluble fullerenes, and the toluene-insoluble fraction was re-suspended in methanol. This suspension was purified using a filtration funnel with an ultrasonic horn driven by 600 W, 20 kHz ultrasonic processor at ~0 C, and methanol was continuously added to maintain a con-

stant filtration volume. This was followed by washing with 6 M sulfuric acid to remove traces of any metal (mostly titanium) introduced into the sample from the ultrasonic horn. Purity greater than 90% was obtained with yields ranging between 30–70%.

Hernadi et al. (1996), reported the use of a combination of ultrasound and various chemical treatments in separating carbon nanotubes from the other impurities from carbon nanotube synthesis by catalytic decomposition of acetylene over supported Co/silica and Fe/silica. Dilute nitric acid (30%) was used to dissolve metallic particle (Co/Fe). Then sample was sonicated in a mixture of *n*-hexane, acetone and isopropanol. The purity and yield of carbon nanotubes generated from this purification technique were not reported.

Mechanical purification

Catalytic metal particles enclosed in carbon nanotube graphitic shells can be removed mechanically based on the ferromagnetic properties of the metal particles. The method of Thien-Nga et al. (2002) mixed SWNT suspension containing metal particles with inorganic nanoparticles in an ultrasonic bath that mechanically separated the ferromagnetic particles from their graphitic shells. The separated ferromagnetic particles were then trapped by permanent magnetic poles followed by a chemical treatment to obtain high purity single walled carbon nanotubes.

Functionalization

This purification technique is based on making single walled carbon nanotubes more soluble than the impurities by attaching functional groups to the nanotubes. The soluble carbon nanotubes can be separated from such insoluble catalytic impurities, and then the functional groups are removed. Georgakilas et al. (2002), described using 1,3-dipolar cycloaddition of azomethineylides in dimethylformamide (DMF) suspension to enhance the solubility of the functionalized single-wall carbon nanotubes while the catalytic metal particles remain insoluble. Amorphous carbon impurities also dissolve in the DMF suspension. The modified carbon nanotubes were separated from the amorphous carbon through a slow precipitation process that took place by adding diethyl ether to a chloroform solution of functionalized single walled carbon nanotubes. This process was repeated three times with the recovered soluble material, and the solid residue, containing the amorphous carbon impurities was discarded. The purified single-wall carbon nanotubes were recovered by thermal treatment at 350 C, which eliminated the functional group attachments, followed by annealing to 900 C. The iron content in the impure single-wall carbon nanotubes and functionalized single-wall carbon nanotubes as measured by atomic absorption analysis was ~26% Fe (w/w) and ~0.4% Fe (w/w), respectively.

Microfiltration

This purification technique is based on size or particle separation that separates single-wall carbon nanotubes from coexisting carbon nanospheres (CNS), metal nanoparticles, polyaromatic carbons and fullerenes. A suspension of single-wall carbon nanotubes, CNS and metal nanoparticles is made using an aqueous solution with a cationic surfactant. The carbon nanotubes are subsequently trapped using a membrane filter, while other nanoparticles (metal nanoparticles and carbon nanospheres) passed through the filter. In this procedure (Bandow et al. 1997) a sample was soaked in organic solvents, such as CS_2, to dissolve and extract polyaromatic carbons and fullerenes. The CS_2 insoluble fractions were then trapped in a filter and then dispersed in an aqueous solution of 0.1% cationic surfactant (benzalkonium chloride) using ultrasonic agitation to separate the CNS and metal particles from the carbon nanotubes. After sonication for 2 h, the suspension was forced through a micro filtration cell using an overpressure (~2 atm) of N_2 gas, and a stirring unit was used to prevent surface contamination of the membrane filter by the unfiltered components. Most of the CNS and metal nanoparticles passed through the filter while the carbon nanotubes and a small amount of residual CNS and metal particles were caught on the filter. The micro filtration process was repeated for three cycles to minimize the amount of residual CNS and metal nanoparticles trapped between the carbon nanotubes ropes. Both the CNS and carbon nanotubes fractions were soaked in ethanol to wash out the surfactant. The suspension (CNS fraction) that passed through the membrane filter was then dried in a rotary evaporator at 60 C. The purity of the carbon nanotubes in the final purified fraction was in excess of 90 wt.%.

Chromatography

This technique is mainly employed in separating small amounts of single-wall carbon nanotubes into fractions with small size (length and diameter) distribution by running single-wall carbon nanotubes over a column with porous material. The columns that have been used include high performance liquid chromatography–size

exclusion chromatography (HPLC–SEC) and gel permeation chromatography (GPC). A review of the chromatography purification technique has been given by Niyogi et al. (2001). The procedure for GPC started with carbon nanotubes functionalized by octadecylamine to be soluble in tetrahydrofuran (THF). Then the solution was run over a gel permeation chromatographic column (Styragel HMW7), with THF as the mobile phase. The chromatogram, obtained using a photodiode array detector (PDA), showed elution of two bands. Of the two main fractions obtained, the first contains semi-conducting single-wall carbon nanotubes, and the second fraction contained nanoparticles and amorphous carbon. It was estimated that 50% of the single-walled carbon nanotubes in the soot was recovered from the first fraction eluted from the column. This technique was said to offer the promise of sorting single walled carbon nanotubes by length, diameter and chirality.

Evaluation of purification methods

The various purification methods combined two or more purification techniques. Typically, an initial mild oxidation step was used to remove amorphous carbon and expose catalyst metal particles to the surface. This was followed by treatment in strong acids to dissolve the catalyst particles or treatment in organic solvents to dissolve fullerenes. The carbon nanotube product was subsequently filtered and washed with alcohol or deionized water to any remove residual acid. The carbon nanotube products were then dried at elevated temperatures (800–1,200 C). Purification techniques can alter the structural surface of the carbon nanotubes according to Ajayan (2000), and caution was recommended when considering purification processes. Purification should remove carbonaceous impurities and the catalyst metal particles with minimal impact on the carbon nanotubes.

Selection of synthesis and purification methods

Laboratory-scale carbon nanotube synthesis techniques used either condensation of a carbon vapor or the catalytic action of transition metal particles on carbon vapor. Typical catalytic transition metals with high carbon nanotube yield were iron, nickel, and cobalt–molybdenum. The catalytic chemical vapor deposition processes appeared to be the most promising for an industrial chemical reactor.

Two catalytic chemical vapor deposition reactors were selected for the conceptual design of carbon nanotube processes. The reactors use the high-pressure carbon monoxide disproportionation reaction over iron catalytic particle clusters (HiPCO reactor), and the catalytic disproportionation of carbon monoxide or hydrocarbon over a silica supported cobalt–molybdenum catalyst (CoMoCAT reactor). Purification of the carbon nanotube product uses a multi-step approach: oxidation, acid treatment, filtration and drying. The oxidation treatment is used to selectively remove amorphous carbon impurities without affecting the structural integrity of the carbon nanotube product.

Conceptual design of carbon nanotube processes

Two processes have been designed, one using the HiPCO reactor and the other using the CoMoCAT reactor. Criteria were low cost, high product yield and selectivity, catalyst performance, and moderate temperatures and pressures. A capacity for the conceptual design was 5,000 metric tons/year which is the size of a carbon nanofiber production plant operated by Grafil, a California-based Mitsubishi Rayon subsidiary (C & E News 2005). Carbon nanotubes will displace carbon fibers in advanced polymer composites, and this plant capacity is comparable to other carbon fiber production facilities (Agboola 2005).

The conceptual designs begin with the development of a process flow diagram (PFD) for the two processes. Then the material and energy balance equations, rate equations and equilibrium relationships are developed for each unit in the PFD. These equations are given by Agboola (2005) and summarized in tabular form for both designs. Material balance equations include the overall material balance and the component material balance equations, and the steady state material balance for a component is written as:

$$F_{\text{inlet}}^{(i)} - F_{\text{outlet}}^{(i)\leftarrow} + F_{\text{gen}}^{(i)} = 0 \qquad (2)$$

where i represents the name of component, and F stands for mass flow rate in kg/h. The overall mass balance is the summation of all component material balances.

The steady state overall energy balance is formulated based on the first law of thermodynamics. Assuming that the changes in kinetic and potential energy are neglected, the energy balance equation is, (Felder and Rousseau 2000)

$$\Delta H = Q - W \qquad (3)\leftarrow$$

where Q is the net heat added to the system; W is the work done by the system on the surroundings; and ΔH is the change in enthalpy between input and output streams. Thus,

$$\Delta H = \sum_{\text{output}} n^{(i)} h^{(i)} - \sum_{\text{input}} n^{(i)} h^{(i)} \quad (4)$$

the reference condition for enthalpy is the elements that constitute the reactants and products at 298 K and the non-reactive molecular species at any convenient temperature. The specific enthalpy $h_k^{(i)}$ of component i, in stream k, can be expressed as a function of temperature (McBride et al. 2002):

$$h_k^{(i)}(T) = R * a_1^{(i)} T + \frac{a_2^{(i)}}{2} T^2 + \frac{a_3^{(i)}}{3} T^3 + \frac{a_4^{(i)}}{4} T^4 + \frac{a_5^{(i)}}{5} T^5 + \frac{b_1^{(i)}}{T} \text{kJ/kg mol} \quad (5)$$

where a_1, a_2, a_3, a_4, a_5 and b_1 are thermodynamic coefficients, T is temperature (K), and R is gas constant (kJ/kg mol K). The enthalpy functions for the component species in the two processes are given by Agboola (2005).

Conceptual design of the CNT-PFR process

This design is based on the high-pressure carbon monoxide (HiPCO) reactor, a plug flow (PFR) reactor developed at Rice University. The HiPCO reactor converts carbon monoxide into single-wall carbon nanotubes and carbon dioxide, at high pressures (30–50 bar), and at temperatures between 1,273 and 1,473 K. Carbon nanotubes and carbon dioxide are produced from carbon monoxide and iron pentacarbonyl catalyst precursor. The overall conversion of carbon monoxide to carbon nanotubes in the HiPCO reactor was 20 mol% (Bronikowski et al. 2001). The process flow diagram is shown in Fig. 3, and the mass flow rates on the PFD are in kg per h. Descriptions of the process units and process streams are given in Tables 1 and 2. The process consists of four sections, which are the feed preparation section, the reactor section, the separation/purification section and the absorber section.

Feed preparation section

The process equipment used in this section includes a mixer (V-101), a gas-fired heater (E-101) and a gas compressor (C-101). The gas streams entering the mixer (V-101) consist of 2,637 kg/h fresh CO (SR01) and 627 kg/h iron pentacarbonyl vapor (SR02). Iron pentacarbonyl is vaporized into the CO stream by passing pure CO stream through a liquid $Fe(CO)_5$-filled bubbler (Nikolaev 2004). The mixer blends the fresh CO feed (SR01) and iron pentacarbonyl vapor (SR02) streams together at 303 K.

The gas stream (SR03) leaving the mixer, which consists of carbon monoxide saturated with iron pentacarbonyl vapor, is sent to the flow reactor (V-102) at 303 K and atmospheric pressure. The unconverted CO reactant is completely recovered and recycled to the reactor from the compressor. The gas compressor (C-101) supplies 12,340 kg/h CO feed recycle (SR04) at 1,323 K and 450 psia.

The CO recycle is passed through two heat exchanger units (E-102 and E-101) successively to increase its temperature. The cross heat exchanger (E-102) increases the temperature of the CO recycle stream from 551 K (SR17) to 707 K (SR18); while the gas-fired heater (E-101) increases the temperature from 707 K (SR18) to 1,323 K (SR04). The sample calculations for the mass flow rates of the iron pentacarbonyl feed, CO feed and CO feed recycle streams are given by Agboola (2005).

Reactor section

The process units used in this section include a high-pressure reactor (V-102), a gas–solid filter (Z-101), the reactor effluent-feed recycle cross heat exchanger (E-102), the waste heat boiler (E-103), and the heat exchanger water cooler 1 (E-104). The mixed gas stream (SR03) containing CO saturated with iron pentacarbonyl vapor, and the CO feed recycle (SR04), from the heater, are passed through the flow reactor (V-102).

In the reactor, the mixed stream (SR03), containing CO and $Fe(CO)_5$, is rapidly mixed and heated with the hot CO feed recycle stream (SR04). The flow reactor is modeled as an isothermal plug-flow reactor at an operating pressure of 450 psia, and operating temperature of 1,323 K, based on laboratory experiments (Nikolaev 2004). Upon heating, the iron pentacarbonyl vapor decomposes to iron atoms and CO according to Eq. 6

$$Fe(CO)_5 \xrightarrow{\text{Heat}} Fe_{(s)} + 5CO_{(g)} \quad (6)$$

the iron formed from the decomposition of the iron pentacarbonyl, nucleates and form iron clusters that initiate the growth of carbon nanotubes in the gas phase, through carbon monoxide disproportionation reaction (Boudouard reaction)

$$xCO_{(g)} \xrightarrow{\text{Fe}} CNT_{(s)} + \frac{x}{2} CO_{2(g)} \quad (7)$$

the stoichiometrically balanced form of Eq. 7 based on a carbon nanotube molecule containing 3,000 carbon atoms is given by Eq. 8 (Scott et al. 2003):

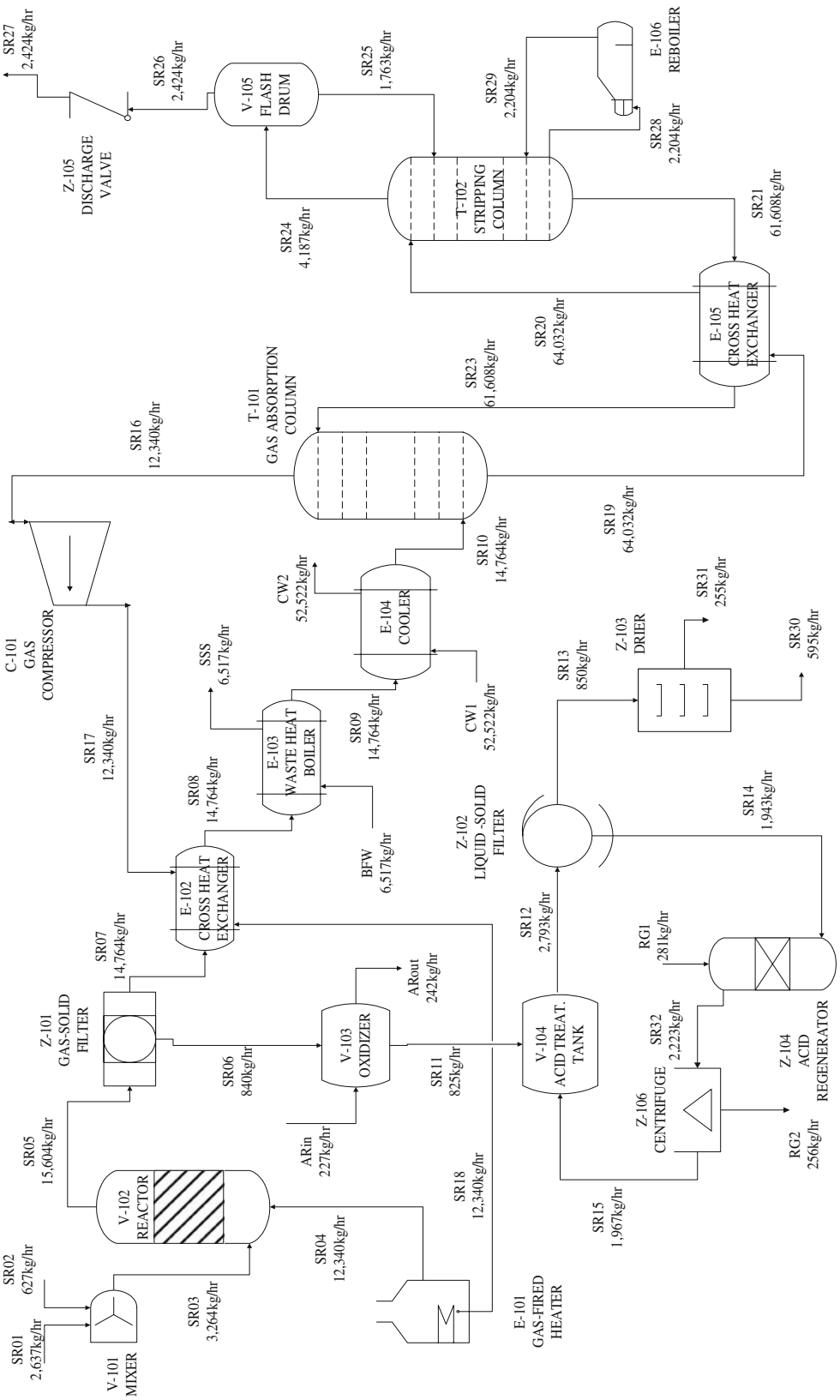

Fig. 3 Process flow diagram for the CNT-PFR design (mass flow rates in kg/h)

Table 1 Process units for the CNT-PFR process model (refer to Fig. 3, the process flow diagram)

Name of unit	Description
Heat exchangers	
E-01	CO Feed recycle gas-fired heater
E-02	Reactor gas effluent-feed recycle cross heat exchanger
E-03	Waste heat boiler
E-04	Heat exchanger water cooler 1
E-05	Solute rich-lean solvent cross heat exchanger
E-06	Kettle reboiler
Process vessels	
V-101	Mixer
V-102	High pressure flow reactor
V-103	Air oxidizer
V-104	Acid treatment tank
V-105	Flash drum
T-101	Gas absorption column
T-102	Gas stripping column
C-101	Gas compressor
Z-101	Gas–solid filter
Z-102	Liquid–solid filter
Z-103	Product drier
Z-104	Acid regeneration column
Z-105	Vent/discharge valve
Z-106	Centrifuge separator

$$6,000CO_{(g)} \xrightarrow{Fe} C_{3,000(s)} + 3,000CO_{2(g)} \quad (8)\leftarrow$$

Carbon nanotubes nucleate and grow in the gas phase on catalytic iron nanoparticle clusters. Growth starts when the catalyst particles are sufficiently large enough for carbon nanotube nucleation; and growth ceases when the catalyst cluster grows too large and prevents the diffusion of additional CO to the particle's surface. The growth of carbon nanotube occurs throughout the length of the reactor. The carbon monoxide disproportionation reaction over iron catalyst is slightly exothermic $\Delta H = -172.5$ kJ/kg mol (Dateo et al. 2002).

In this design, the conversion of CO in the flow reactor to form carbon nanotube, based on Eq. 8, is 20 mol%, i.e., 0.20 kg mol CO reacted to form CNT per kg mol CO fed to the reactor. The conversion used is based on the optimal conversion obtained in the laboratory-scale HiPCO reactor (Davis 2005). The selectivity of the CO reactant to form carbon nanotubes, based on Eq. 8, is 90%, i.e., 0.9 kg mol CO reacted to form carbon nanotube per kg mol CO reacted.

Amorphous carbon is formed in the reactor according to Eq. 9:

$$2CO_{(g)} \rightarrow C_{(s)} + CO_{2(g)} \quad (9)\leftarrow$$

the selectivity of the CO reactant to form amorphous carbon, based on Eq. (8) is 10%, i.e., 0.1 kg mol CO reacted to form amorphous carbon per kg mol CO reacted. The selectivity values used in the HiPCO reactor are based on high TEM studies, which revealed that carbon nanotubes produced by the HiPCO reactor contain lower amorphous carbon over coating in contrast to carbon nanotubes produced by the laser vaporization or arc discharge processes (Bronikowski et al. 2001).

The effluents stream (SR05) from the reactor contains carbon nanotube (CNT), amorphous carbon, iron particles, CO_2 and unconverted CO. The carbon nanotube formed contains residual iron particles from the thermal decomposition of iron pentacarbonyl. The carbon nanotube produced is transported out of the flow reactor by the continuous gas flow and sent to a gas–solid filter (Z-101). The gas–solid filter separates the solid products (SR06) containing carbon nanotube, residual iron and amorphous carbon from the hot, mixed carbon monoxide and carbon dioxide gas stream (SR07). It is essential to remove 99.999% solids upstream of the compressor, in order to minimize erosion of turbine.

The hot, mixed-gas stream (SR07) from the gas–solid filter (Z-101) is initially cooled in the reactor-effluent/feed-recycle cross heat exchanger (E-102). The cross heat exchanger cools the gas stream from 1,323 (SR07) to 1,223 K (SR08), and preheats the CO feed recycle stream from 551 (SR17) to 707 K (SR18). The mixed gas stream (SR08) from the cross heat exchanger is then passed to the waste heat boiler (E-103).

The waste heat boiler (E-103) cools the mixed gas stream from 1,223 (SR08) to 573 K (SR09) by removing heat from the mixed gas stream to produce saturated steam. Boiler feed water (BFW) is supplied to the waste heat boiler (E-103) at 303 K, while saturated steam (SSS) is produced at 533 K and 675 psia. The saturated steam produced is used for process heating in other process units such as the reboiler and heater.

The gas stream exiting the waste heat boiler is further cooled from 573 (SR09) to 330 K (SR10) in the heat exchanger water cooler 1 (E-104). Cooling water is supplied to the heat exchanger cooler at 303 K (CW1) and exits at 323 K (CW2). The gas stream leaving the water cooler (SR10) is then fed into the gas absorption column (T-101) as bottoms at 330 K.

Separation/purification section

The process units used in the separation/purification section include the previously described gas–solid filter (Z-101), an air oxidizer (V-103), an acid treatment tank (V-104), a liquid–solid filter (Z-102), a product drier (Z-103), an acid regeneration column (Z-104) and a

Table 2 Process streams in the CNT-PFR process model (Refer to Fig. 3)

Name of stream	Description of process streams
SR01	Fresh CO feed to mixer (V-101)
SR02	Iron pentacarbonyl vapor to mixer (V-101)
SR03	Mixed CO and $Fe(CO)_5$ feed to reactor (V-102)
SR04	CO feed recycle from heater (E-100) to reactor (V-102)
SR05	Effluent stream from reactor (V-102) to filter 1 (Z-101)
SR06	Carbon nanotube from filter 1 (Z-101) to oxidizer (V-103)
SR07	Gas stream from filter 1 (Z-101) to heat exchanger (E-102)
SR08	Mixed gas stream from E-102 to waste heat boiler (E-103)
SR09	Mixed gas stream from E-103 to cooler 1 (E-104)
SR10	Gas stream from cooler 1 (E-104) to gas absorber (T-101)
SR11	Carbon nanotube from V-103 to acid treatment tank (V-104)
SR12	Carbon nanotube slurry from V-104 to filter 2 (Z-102)
SR13	Carbon nanotube from filter 2 (Z-102) to drier (Z-103)
SR14	Acid stream from filter 2 (Z-102) to regenerator (Z-104)
SR15	Acid stream from centrifuge (Z-106) to acid tank (V-104)
SR16	CO gas stream from absorber (T-101) to compressor (C-101)
SR17	CO recycle from compressor (C-101) to exchanger (E-102)
SR18	CO recycle from exchanger (E-102) to heater (E-101)
SR19	CO_2-rich MEA solution from T-101 to exchanger (E-105)
SR20	CO_2-rich solution from E-105 to stripping column (T-102)
SR21	Lean MEA solution from T-102 to exchanger (E-105)
SR23	Lean MEA solution from E-105 to gas absorber (T-101)
SR24	CO_2 vapor from T-102 to flash drum (V-105)
SR25	Recovered MEA solution from V-105 to stripper (T-102)
SR26	CO_2 gas from flash drum (V-105) to vent valve (Z-105)
SR27	CO_2 Gas from Z-105 to other processes
SR28	Lean MEA solution from stripper (T-102) to reboiler (E-106)
SR29	MEA vapor from E-105 to stripping column (T-102)
SR30	Carbon nanotube from product drier (Z-103) to storage or sales
SR31	Water evaporated from carbon nanotube product from Z-103
SR32	Mixed product stream from Z-104 to centrifuge (Z-106)
Utility streams	
CW1	Cooling water inlet stream of heat exchanger cooler 1 (E-104)
CW2	Cooling water outlet stream of heat exchanger cooler 1 (E-104)
BFW	Boiler feed water to waste heat boiler (E-103)
SSS	Saturated steam from boiler (E-103) to reboiler (E-106)
ARin	Air inlet stream to oxidizer (V-103)
ARout	Air outlet stream from oxidizer (V-103)
RG1	Fresh feed to the acid regeneration column (Z-104)
RG2	Waste stream from centrifuge separator (Z-106)

centrifuge separator (Z-106). These process units are used to separate and purify the carbon nanotube product from impurities such as amorphous carbon and iron nanoparticles.

The gas–solid filter (Z-101) separates the carbon nanotubes product from the hot gas effluent stream from the reactor. The carbon nanotubes are collected as solid residues on the surfaces of the gas–solid filter as the reactor effluent stream (SR05) flows through the filter. The solid product (SR06) collected on the filter surface contains carbon nanotubes, amorphous carbon and residual iron particles. Consequently, additional purification steps are required to remove the amorphous carbon and residual iron particle impurities from the carbon nanotube product.

The purification of the carbon nanotube product in the CNT-PFR process involves a multi-step approach: oxidation, acid treatment, filtration and drying. The purification section consists of an oxidizer (V-103), in which a heated air gas stream is passed over the carbon nanotube product (SR06) collected from the filter (Z-101). The oxidation treatment is used to selectively remove amorphous carbon impurities without affecting the structural integrity of the carbon nanotube product.

In addition to the removal of amorphous carbon, the oxidation step exposes the iron nanoparticles embedded in the outer carbon layers to the nanotube surface and oxidizes the iron particles to iron oxide (Chiang et al. 2001a). Consequently, the encased iron particles, hitherto impervious to dissolution in acid solution, are easily extracted as soluble iron oxides by treatment in concentrated hydrochloric acid.

In the acid treatment tank (V-104), the oxidized carbon nanotube product (SR11) containing iron oxi-

des, is treated with 12% hydrochloric acid (HCl) solution (Meyyappan 2004). The iron oxide dissolves in the acid solution to form iron chloride ($FeCl_2$) and water. The ratio of the amount of iron oxide removed to the amount of HCl used is based on the reaction between iron oxide and HCl solution. However, since organometallics [$Fe(CO)_5$] are used to nucleate the carbon nanotubes produced, there will be some iron particles in the CNT-PFR carbon nanotube final product. The final carbon nanotube product will contain 97 mol% carbon nanotubes and 3 mol% iron (Bronikowski et al. 2001).

The nanotube slurry (SR12), containing the dissolved iron chloride, and carbon nanotubes is sent to the liquid–solid filter (Z-102), which separates the purified carbon nanotube product (SR13) from the iron chloride solution (SR14). The carbon nanotubes collected on the filter surface are washed several times with deionized water to remove any trace of hydrochloric acid from the carbon nanotube product. The washed, filtered and purified carbon nanotube product (SR13) is then dried at 800 K in the product drier (Z-103). The final carbon nanotube product (SR30), from the drier, is then sent to storage for packaging and sales.

The iron chloride solution (SR14) from the liquid–solid product filter is sent to an acid regeneration column (Z-104), where the hydrochloric acid solution is regenerated. The iron chloride solution is oxidized in the column to produce hydrochloric acid and iron oxide residue. The iron oxide residue produced is saturated with hydrochloric acid and is removed from the acid solution in the centrifuge separator (Z-106) which is sent to off-site treatment (http://www.acidrecovery.com). The recovered hydrochloric acid (SR15) from the centrifuge is recirculated back to the acid treatment tank (V-104) for another reaction cycle.

Absorber section

The process units in the absorber section include: a gas absorber (T-101), a gas stripping column (T-102), and a cross heat exchanger (E-105). Other process units include a kettle reboiler (E-106), a flash drum (V-105) and a discharge/vent valve (Z-105). The carbon dioxide produced during the CO disproportionation reaction over catalytic iron nanoparticles is absorbed in the counter-current flow of monoethanol amine (MEA) solution in the gas (CO_2) absorption column.

The mixed gas stream (SR10) from the heat exchanger water cooler (E-104), containing CO_2 and unconverted CO, enters the gas absorption column as bottoms feed at 330 K and 75 psia. The carbon dioxide is absorbed in the counter-current flow of monoethanol amine solution (SR23) fed into the absorption column at the top. The gas stream exiting the gas absorber at the top (SR16) contains unconverted CO from the reactor.

The CO feed recycle stream (SR16) recovered from the gas absorption column is not at the same pressure as the reaction pressure (450 psia), due to pressure losses at the filter, reactor, and flow losses. The CO feed recycle stream is passed through a gas compressor (C-101). The gas compressor increases the pressure of the CO feed recycle stream by adiabatic compression from 75 psia (SR16) to 450 psia (SR17).

The CO_2-rich monoethanol amine (MEA) solution (SR19) leaves the gas absorption column at the bottom at 330 K and enters the solute rich-lean solvent cross heat exchanger (E-105). The cross heat exchanger preheats the CO_2-rich MEA solution from 330 (SR19) to 393 K (SR20). The cross heat exchange occurs between the solute-rich MEA solution (SR19) and the lean MEA bottoms stream (SR21) from the stripping column.

The preheated solute-rich monoethanol amine liquid stream (SR20) enters the gas stripping column (T-102) at the top. Carbon dioxide gas is stripped from the solute-rich monoethanol amine solution in the column by steam stripping. Saturated steam is supplied to the reboiler (E-106) for gas stripping from the waste heat boiler (E-103).

The gas stripped (SR24) from the stripping column containing CO_2 and water vapor is sent to the flash drum (V-105), where the aqueous fraction liquid carryover (SR25) is recovered and returned to the stripping column. The carbon dioxide gas stream (SR26) separated in the flash drum is either transferred from the plant to other carbon dioxide consuming processes, or discharged from the plant in form of flue gas (SR27), as long as emission standards are met. The backpressure control valve (Z-105) controls the CO_2 emission and discharge from the production plant.

The lean monoethanol amine solution (SR21) recovered in the stripping column leaves the gas stripper at the bottom, and exchanges heat with the CO_2-rich monoethanol amine solution (SR19) from the gas absorption column in the cross heat exchanger (E-105). The lean MEA solution from the stripping column enters the cross heat exchanger (E-105) at 393 K (SR21) and leaves at 330 K (SR23).

Equipment and flow summary tables

The equipment and flow utilities summary are given by Agboola (2005). These are from the solution of the process model equations.

Conceptual design of the CNT-FBR process

This design is based on carbon monoxide disproportionation over mixed cobalt–molybdenum catalyst on silica support in a fluidized bed reactor developed at the University of Oklahoma. The reaction forms carbon nanotubes and carbon dioxide at temperatures between 973 and 1,223 K, and total pressure ranging from 15 to 150 psia. The conversion of CO is 20 mol%, and the carbon monoxide selectivity is 80% (Resasco et al. 2001). The process flow diagram for the CNT-FBR process is shown in Fig. 4, and the mass flow rates on the PFD are in kg per h. The descriptions of the process units and streams in the process flow diagram are given in Tables 3 and 4. The process consists of the feed preparation section, the reactor section, the absorber section and the separation/purification section.

Feed preparation section

The process units in the feed preparation section include the heater (E-201) and the gas compressor (C-201). Fresh CO feed stream (SR01) at 303 K is combined with the CO feed recycle stream (SR17) at 490 K in the gas-fired heater (E-201). The make-up CO feed stream (SR01) consists of 3,471 kg/h of CO at 490 K, while the gas compressor (C-201) supplies 13,883 kg/h of CO feed recycle (SR17) to the heater at 490 K and 150 psia. The combined CO feed stream (SR02) is fed into the fluidized bed reactor (V-201) at 1,223 K and 150 psia. The temperature of the combined CO feed stream (SR02) leaving the heater is at 1,223 K, and the stream is sent to the reactor (V-201). The operating conditions in the reactor are maintained at 1,223 K and 150 psia, based on the experimental conditions in the laboratory-scale CoMoCAT process.

Reactor section

The reactor section consists of a fluidized bed reactor (V-201), the cyclone separator (Z-201), the gas–solid filter (Z-202), the waste heat boiler (E-202) and the heat exchanger water cooler (E-203). In the fluidized bed reactor, the combined CO feed stream (SR02) from the heater is reacted on silica-supported bimetallic cobalt–molybdenum catalysts (SR11), at operating temperature and pressure of 1,223 K and 150 psia. Carbon nanotubes are formed by the CO disproportionation over Co–Mo catalysts, according to the Boudouard reaction, Eq. 7. The stoichiometrically balanced form of Eq. 7 based on a carbon nanotube molecule containing 3,000 carbon atoms is given by Eq. 10.

$$6,000\mathrm{CO}_{(g)} \xrightarrow{\mathrm{SiO_2/Co/Mo}} \mathrm{C}_{3,000(s)} + 3,000\mathrm{CO}_{2(g)} \quad (10)\leftarrow$$

In this design, the conversion of CO in the fluidized bed reactor to form carbon nanotube, based on Eq. 9, is 20 mol%, i.e., 0.20 kg mol CO reacted to form CNT per kg mol CO fed to the reactor. The carbon monoxide selectivity to form carbon nanotubes, based on Eq. 10, is 80%, i.e., 0.8 kg mol CO reacted to form CNT per kg mol CO reacted (Resasco et al. 2001).

Amorphous carbon is formed in the fluidized bed reactor (V-201) according to Eq 9. The selectivity of the CO reactant to form amorphous carbon, based on Eq. 9 is 20%, i.e., 0.2 kg mol CO is converted to CNT per kg mol CO reacted.

The effluent stream (SR03) from the reactor contains carbon nanotubes and amorphous carbon, grown and attached to the silica-supported bimetallic catalysts, carbon dioxide and unconverted carbon monoxide. The effluent stream is initially passed through a cyclone separator (Z-201). The cyclone separates the solid catalyst particles (SR05) from the hot mixed-gas stream (SR04).

The gas stream from the cyclone, containing CO, CO_2, and solid catalyst particle carryover, is passed through a gas–solid filter (Z-202) to remove any solid catalyst entrainments from the gas stream. The entrained solids (SR12) collected by the filter are sent to the alkali-leaching tank (V-202).

The hot, gas stream (SR13) from the gas–solid filter (Z-202) is sent through a waste heat boiler (E-202). The waste heat boiler cools the mixed-gas stream from 1,223 K (SR13) to 573 K (SR14). In the process, boiler feed water supplied at 303 K (BFW) is converted to saturated steam at 533 K (SST). The saturated steam produced in the waste heat boiler is used for steam stripping in the stripping column and/or for other heating requirements.

The mixed-gas stream (SR14) leaving the waste heat boiler is passed into the water cooler (E-203), where water cools the mixed-gas stream from 573 (SR14) to 330 K (SR15), the required inlet temperature of the gas absorber. Cooling water is supplied to the cooler at 303 K (CW5), and leaves the water cooler at 323 K (CW6). The mixed gas stream from the water cooler (SR15), is fed to the gas absorber (T-201) bottom at 330 K.

Separation/purification section

The carbon nanotubes produced in the fluidized bed reactor are grown on and remain attached to the silica-supported bimetallic catalysts. In order to separate and

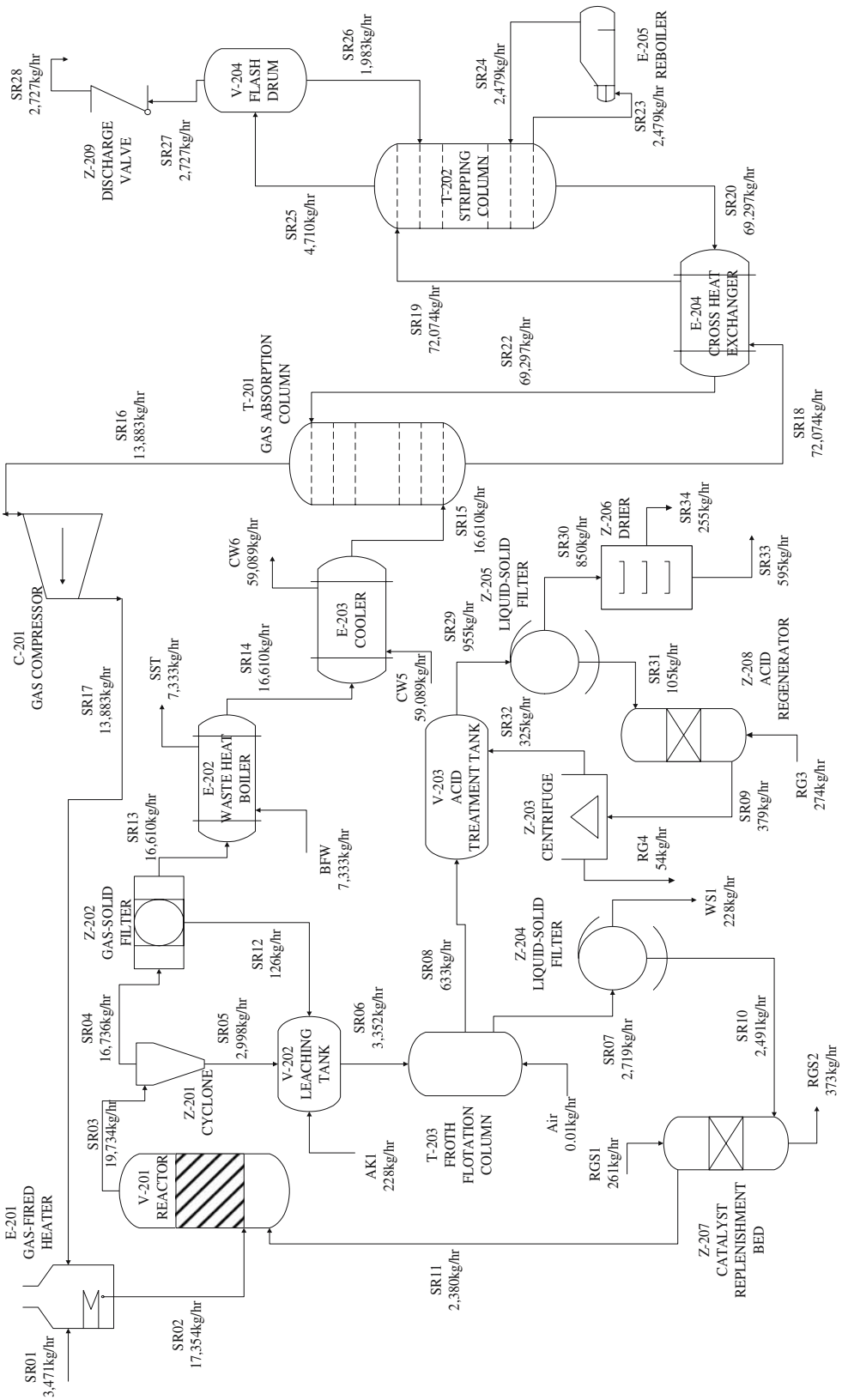

Fig. 4 Process flow diagram for the CNT-FBR design (mass flow rates in kg/h)

purify the carbon nanotube product from the silica-supported, cobalt–molybdenum bimetallic catalysts, the froth flotation purification process is employed.

The process involves the use of inorganic surfactant, and air as a medium of separating the carbon nanotube from the silica-supported bimetallic catalysts. The

Table 3 Process units for the CNT-FBR process (Refer to Fig. 4)

Name of unit	Process unit description
Heat exchangers	
E-201	CO feed and recycle gas-fired heater
E-202	Waste heat boiler
E-203	Heat exchanger water cooler 1
E-204	Solute rich-lean solvent cross heat exchanger
E-205	Kettle reboiler
Process vessels	
V-201	Fluidized bed reactor
V-202	Alkali leaching tank
V-203	Acid treatment tank
V-204	Flash drum
T-201	Gas absorption column
T-202	Gas stripping column
T-203	Froth flotation column
C-201	Gas compressor
Z-201	Cyclone separator 1
Z-202	Gas–solid filter
Z-203	Centrifuge separator
Z-204	Liquid–solid filter 1
Z-205	Liquid–solid filter 2
Z-206	Product drier
Z-207	Catalyst replenishment bed
Z-208	Acid regeneration column
Z-209	Discharge valve

purity of carbon nanotubes produced by the froth flotation process is 80% (Pisan et al. 2004). The carbon nanotubes still contain residual metal particles after the flotation process, additional purification steps are required to increase the purity of the final product closer to 100%.

The carbon nanotube product, containing residual Co and Mo particles, is dissolved in 12% hydrochloric acid (HCl) solution. The ratio of the amount of residual Co and Mo metals removed to the amount of HCl used is based on the reaction between the residual Co/Mo metals and HCl. The treatment of the nanotubes product in 12% HCl improves the purity of the final nanotube product to 97 mol% CNT (Resasco et al. 2001).

The silica-supported solid catalyst (SR05) from the cyclone separator (Z-201) is sent to the alkali-leaching tank (V-202), where it is washed with 2 M sodium hydroxide solution (Resasco et al. 2001). The sodium hydroxide solution (AK1) is used to break the carbon nanotubes-supported catalysts interaction by silica leaching. The treatment with sodium hydroxide breaks the carbon nanotube-silica attachments, without removing the cobalt–molybdenum metals present on the silica substrate.

The carbon nanotube slurry (SR06) from the alkali leaching tank, which contains the detached carbon nanotubes, silica supports, residual cobalt and molybdenum metals, is passed into the froth flotation column (T-203), filled with an organic surfactant. Typical organic surfactants used in the froth flotation purification process include non-ionic surfonic-24-7 (Pisan et al. 2004).

Air is used as a medium of separation in the froth floatation column, such that air bubbled through the column at rates high enough, traps the carbon nanotubes at the air–water interface as a result of the reduced surface tension at the surfactant surface. Carbon nanotubes (SR08), trapped at the air–water interface, and washed with deionized water, is separated from the surfactant and sent to an acid treatment tank (V-203).

The residual metal catalytic particles in the carbon nanotube product from the froth flotation column is dissolved and extracted with 12% hydrochloric acid solution (SR32). In the acid treatment tank, the residual cobalt and molybdenum catalysts react with hydrochloric acid solution to form soluble cobalt chloride and molybdenum chloride, respectively. The carbon nanotube slurry (SR29) is then passed through a liquid–solid filter (Z-205). The liquid–solid filter separates the purified carbon nanotube product (SR30) from the liquid stream (SR31).

The carbon nanotube product (SR30) is then sent to the product drier (Z-206), where it is annealed at 800 K. The purity of the final carbon nanotubes product, obtained after acid dissolution and filtration, is 97 mol% carbon nanotubes, 1.5 mol% cobalt metal and 1.5 mol% molybdenum metal particles (Resasco et al 2001). The final carbon nanotube product (SR33), from the drier, is then sent to storage for packaging and/or sales.

The liquid stream (SR31) from the filter (Z-205) is sent to an acid regeneration column (Z-208), where hydrochloric acid is recovered from the metal chloride solution. Hydrochloric acid is regenerated from the oxidation of the metal chlorides solution in the acid regenerator column. The cobalt and molybdenum oxides produced in the acid regenerator are removed from the hydrochloric acid in the centrifuge separator (Z-203). The recovered acid solution is subsequently recycled to the acid treatment tank (V-203) for another reaction cycle.

The silica-supported catalysts slurry (SR07) from the froth flotation column is passed through another liquid–solid filter (Z-204), where the spent, supported catalyst particles are collected. The spent, supported catalyst particles (SR10) collected on the filter, are sent to a catalyst regeneration bed (Z-207) for catalyst regeneration.

Table 4 Process Streams in the CNT-FBR Process (Refer to Fig. 4)

Stream	Process stream description
SR01	Fresh CO feed stream to mixer/heater (E-201)
SR02	Combined CO feed stream from heater (E-201) to reactor (V-201)
SR03	Effluent stream from reactor (V-201) to cyclone (Z-201)
SR04	Mixed gas stream from cyclone (Z-201) to filter 1(Z-202)
SR05	Solids from cyclone (Z-201) to alkali leaching tank (V-202)
SR06	Nanotube slurry from tank (V-202) to flotation column (T-203)
SR07	Effluent stream containing catalysts from T-203 to filter 2 (Z-204)
SR08	Carbon nanotube froth from T-203 to acid dissolution tank (V-203)
SR09	Mixed stream from acid regenerator (Z-208) to centrifuge (Z-203)
SR10	Spent catalysts from filter 2 (Z-204) to regeneration bed (Z-207)
SR11	Fresh Co–Mo catalysts from bed (Z-207) to reactor (V-201)
SR12	Entrained solids from filter 1 (Z-202) to leaching tank (V-202)
SR13	Mixed gas stream from filter 1 (Z-202) to waste heat boiler (E-202)
SR14	Mixed gas stream from E-202 to water cooler 1 (E-203)
SR15	Gas stream from cooler 1 (E-203) to gas absorber (T-201)
SR16	CO recycle stream from absorber (T-201) to gas compressor (C-201)
SR17	CO feed recycle from compressor (C-201) to heater (E-201)
SR18	CO_2-rich amine (MEA) solution from T-201 to exchanger (E-204)
SR19	CO_2-rich MEA solution from e-204 to stripping column (T-202)
SR20	Lean MEA solvent from stripper (T-202) to exchanger (E-204)
SR22	Lean MEA solvent from exchanger (E-204) to absorber (T-201)
SR23	Lean MEA solvent from stripper (T-202) to reboiler (E-205)
SR24	MEA vapor from reboiler (E-205) to gas stripper (T-202)
SR25	Stripped CO_2 vapor from stripper (T-202) to flash drum (V-204)
SR26	Recovered MEA solvent from flash drum (V-204) to stripper (T-202)
SR27	CO_2 gas stream from flash drum (V-204) to vent valve (Z-209)
SR28	CO_2 gas discharge from valve (z-209) to other processes
SR29	Carbon nanotube slurry from acid tank (V-203) to filter 3 (Z-205)
SR30	Carbon nanotube product from Z-205 to product drier (Z-206)
SR31	Mixed stream from filter (Z-205) to acid regenerator (Z-208)
SR32	Recovered acid from centrifuge (Z-203) to acid tank (V-203)
SR33	Carbon nanotube from product drier (Z-206) to storage/packaging/sales
SR34	Water evaporated from nanotube product in drier (Z-206)
Utility streams	
AK1	Sodium hydroxide feed into alkali leaching tank (V-202)
RGS1	High pressure steam to catalyst regeneration bed (Z-207)
RG4	Co and Mo oxide residues from centrifuge separator (Z-203)
BFW and SST	Feed water and saturated steam to and from waste heat boiler (E-202)
CW5 and CW6	Cooling water inlet and outlet streams for the water cooler 1 (E-203)
WS1	Waste stream from liquid–solid filter 2 (Z-204)
Air	Air feed to froth flotation column (T-203)

The catalysts are replenished by adding cobalt and molybdenum particles to make up for the cobalt and molybdenum losses in the final product and during the acid purification step. The regenerated catalysts (SR11) are then recycled back into the fluidized bed reactor for another reaction cycle.

The waste stream (WS1) from the liquid–solid filter (Z-204), which contains process fluids, such as the organic surfactant, and sodium hydroxide, is sent to a solvent recovery unit, where the organic surfactant is recovered and recycled for re-use.

Absorber section

In the absorber section, the carbon dioxide in the bottoms feed (SR15), from the water cooler, is absorbed in the counter-current flow of monoethanol amine solution (SR22) fed in at the top of the absorption column. The unconverted CO gas stream (SR16) which is not absorbed, leaves the gas absorber at the top and is sent to the gas compressor (C-201). The gas compressor increases the CO recycle gas pressure from 75 psia (SR16) to 150 psia (SR17). The CO feed recycle is subsequently recirculated to the gas-fired heater (E-201), where it is combined with fresh CO feed (SR01) and heated to 1,223 K.

The solute-rich MEA solution (SR18) leaving the gas absorber at the bottom is passed to the solute-rich-lean solvent cross heat exchanger (E-204), where it is preheated by the lean MEA solution (SR20) recovered from the stripping column. The cross heat exchange occurs between the solute-rich MEA solution (SR18) and the lean monoethanol amine solution (SR20) from the stripping column. The solute-rich MEA solution

(SR19) enters the top of gas stripping column (T-202) at 393 K. Carbon dioxide gas is steam stripped from the solute-rich solution in the gas stripper. Saturated steam is supplied to the reboiler (E-205) for gas stripping from the waste heat boiler (E-202).

The carbon dioxide (SR25) thus stripped, leaves the stripping column at the top and is sent to the flash drum (V-204) where any liquid entrainment in the vapor stream is recovered and returned to the gas stripping column. The CO_2 gas stream (SR27) which is flashed and separated in the flash drum, is either transferred from the carbon nanotube process to other carbon dioxide consuming processes, or discharged from the plant in form of flue gas (SR28), as long as emission standards are met. The backpressure control valve (Z-209) discharges the carbon dioxide from the plant.

The lean monoethanol amine solution (SR20) recovered in the gas stripping column leaves the stripping column at the bottom and exchanges heat with the solute-rich monoethanol amine solution (SR18), from the gas absorption column, in the cross heat exchanger (E-204). The lean monoethanol amine solution enters the cross heat exchanger at 393 K (SR20) and leaves at 330 K (SR22).

Equipment and flow summary tables

The equipment and flow utilities summary are given by Agboola (2005). These are from the solution of the process model equations.

Summary and comparison of the conceptual designs

The conceptual designs of two carbon nanotube production processes are summarized in Tables 5 and 6. A production capacity of 5,000 metric tons of carbon nanotubes per year (595 kg/h) is comparable to a plant producing carbon fibers for composites. In the CNT-PFR process, iron carbonyl and carbon monoxide were reacted in a plug flow reactor (PFR) at 1,050 C and 450 psi with a selectivity of 90% to single wall carbon nanotubes. Purification steps included oxidation, acid treatment and filtration. In the CNT-FBR process, carbon monoxide was reacted over a cobalt molybdenum catalyst in a fluidized bed reactor (FBR) at 950 C and 150 psi with a selectivity of 80% to single wall carbon nanotubes. Purification steps included oxidation leaching, froth flotation and acid treatment. The types of process equipment used in each plant are listed in Table 6 for the process flow diagrams shown in Figs. 3 and 4.

The raw materials, products, energy requirements and the emissions from the two processes are compared in Tables 7 and 8. The total flow rate of raw materials, which consisted of the feed and other reactants into the CNT-PFR and CNT-FBR processes, was 3,772 and 4,234 kg/h to produce 595 kg/h of carbon nanotubes. The energy consumed by the processes was from steam, natural gas and electricity. The steam consumed by the two processes was comparable 2,565 and 2,885 kg/h. The electrical energy consumed by the CNT-PFR process (1,056 kW) was significantly higher than the electrical energy consumed by the CNT-FBR process (387 kW) because of the higher operating pressure of the CNT-PFR process (450 psia) compared to the operating pressure of the CNT-FBR process (150 psia).

Economic analysis for the CNT-PFR and CNT-FBR processes

Economic decision analysis was used to estimate the profitability based on the total capital cost and total product cost for the CNT-PFR and CNT-FBR processes. The total plant cost or total capital investment for a chemical process plant consists of the installed equipment costs, offsite facilities costs, start-up costs and the working capital for the plant. The total product cost is an estimate of the annual manufacturing costs and general expenses or sales related costs.

Total plant cost

The installed equipment costs were estimated by CAPCOST, a computer program that uses the equipment module approach for capital cost estimation (Turton et al. 1998). The offsite facilities (30%), start-up costs (10%) and working capital (15%) for the plant design were estimated as a percentage of the installed

Table 5 Summary of the conceptual designs of CNT processes

	CNT PFR process	CNT-FBR process
Catalyst	Fe $Fe(CO)_5 \rightarrow Fe + 5CO$	Co–Mo Silica
Reactants	CO and $Fe(CO)_5$	CO
Reactor type	Plug flow reactor	Fluidized bed
Reactor conditions	1,050 C @ 450 psia	950 C @ 150 psia
Selectivity to CNT	90%	80%
Purification	Oxidation Acid treatment Filtration	Leaching Froth flotation Acid treatment
Production rate (kg/h)	595	595

Table 6 Summary of the process units used in the conceptual designs of CNT processes

Section	CNT-PFR process	CNT-FBR process
Feed preparation	Mixer, heater	Mixer/heater
	Gas compressor	Gas compressor
Reaction	Flow reactor	Fluidized bed
	Heat exchangers	Heat exchangers
Purification	Filters	Filters
	Oxidizer	Flotation column
	Drier/annealer	Drier/annealer
	Centrifuge	Cyclone separator
CO Recycle	Gas absorber	Gas absorber
	Gas stripper	Gas stripper

Table 7 Reactants, products and emissions for the CNT-PFR process

Feed	kg/h	Other	kg/h	Product	kg/h	Emissions	kg/h
CO	2,637	O_2	253	CNT	595	$FeCl_2$	0.07
$Fe(CO_5)$	627	H_2O	255			CO_2	2,666
						Fe_2O_3	256
						H_2O	255
Total mass flow		3,772 kg/h		Total mass flow		3,772 kg/h	
Energy requirements							
Steam		Natural Gas		Electricity			
2,565 kg/h		486 kg/h		1,056 kW			

Table 8 Reactants, products and emissions for the CNT-FBR process

Feed	kg/h	Others	kg/h	Product	kg/h	Emissions	kg/h
CO	3,471	O_2	9	CNT	595	Co_2	2,727
Mo	19	H_2O	488	$CoCl_2$	0.05	Co_2O_3	26
Co	19	NaOH	228	$MoCl_2$	0.04	MoO_3	28
				H_2O	255	NaOH	228
				H_2	25	CO	349
Total mass Flow		4,234 kg/h		Total mass flow		4,324 kg/h	
Energy requirements							
Steam		Natural gas		Electricity			
2,885 kg/h		486 kg/h		387 kW			

equipment cost. The offsite facilities costs included auxiliary or non-processing facilities, and working capital is the money available to sustain the production operation in times of negative cash flow. Start-up costs refer to the cost of plant start-up and bringing it to rated production capacity.

The installed equipment costs for the carbon nanotube production processes were based on the equipment shown in the CNT-PFR and CNT-FBR process flow diagrams in Figs. 3 and 4 and process units in Tables 1 and 3. Equipment not in the CAPCOST program was added as user equipment, and these costs were obtained from the literature. The total capital cost estimates were based on the chemical engineering plant cost index (CEPCI-2005 value) CEPCI = 468, (Chemical Engineering 2005). The total plant cost estimates for the two processes are given by Agboola (2005). The total capital investment (TCI) or total plant costs for the CNT-PFR process was $4.6 million. The total capital investment (TCI) or total plant cost for the CNT-FBR process is $4.4 million.

Total product cost

The total product cost includes the manufacturing costs and general expenses or sales related costs. The manufacturing costs are the expense of producing the product and include direct and indirect manufacturing expenses. The direct manufacturing costs include raw material costs, utilities costs, and labor costs and are estimated using the results from the material and energy balances. Indirect manufacturing expenses includes plant overhead costs, property insurance, environmental costs, etc. and are estimated as a percentage of the labor costs, plant costs and sales revenue. General expenses or sales related costs include administrative costs, distribution and marketing costs, research and development costs. They are relatively constant and are between 20 and 30% of the direct production costs.

Details of the evaluation of the total product cost are given by Agboola (2005). The total product cost for the CNT-PFR process was $187 million which included raw materials costs ($140 million), utilities costs ($2.4 million), operating labor costs ($12 million), capital related costs ($1.2 million) and sales related costs ($31 million). The total product cost for the CNT-FBR process was $124 million which included raw materials costs ($84 million), utilities costs ($2.5 million), labor costs ($16 million), capital related costs ($1.1 million) and sales related costs ($21 million).

Profitability analysis

The net present value (NPV), rate of return (ROR) and economic price were evaluated for the profitability analysis. The net present value is the sum of all of the cash flows for the project discounted to the present value, using the company's minimum attractive rate of return (MARR), and the capital investment required. The rate of return is the interest rate in the net present value analysis that gives a zero net present value. The

economic price is estimated from the total product cost C_T, the annual cost of capital, EUAC annual capital expenditures C_{cap}, and production rate.

The net present value is used to compare similar projects that are competing for capital. The rate of return is used to compare alternate investment opportunities. The economic price is the price required to sell a product in order to make the minimum attractive rate of return.

The economic life of a plant is estimated based on the length of time that the plant can be operated profitably. New more efficient technology, new environmental restrictions or a new product from another process that displaces the current product will end the economic life of the plant. The economic life of 10 years for the two processes was based on the IRS guidelines for the write-off life of plant equipment which was about 10 years. The straight-line method for depreciation with no salvage value was incorporated in the evaluations.

A summary is given in Table 9 of the profitability analysis for the conceptual designs of the CNT processes. Referring to this table, the net present value for the CNT-PFR process was \$609 million as compared to \$753 million for the CNT-FBR process. The rate of return (ROR) based on an economic life of 10 years ($n = 10$) for the CNT-PFR process was 37.4% as compared to 48.2% for the CNT-FBR process. The economic price for carbon nanotubes produced by the CNT-PFR process was \$38 per kg as compared to \$25 per kg for the CNT-FBR process. Based on these results, the CNT-PFR process has the advantage of a higher net present value and lower economic price. The total plant costs are comparable, \$4.6 versus \$4.4 million, but raw materials cost for the CNT-FBR is significantly less than the CNT-PFR, \$140 versus \$84 million (Agboola 2005). This difference is in the cost of iron pentacarbonyl, an expensive raw material at \$26.40 per kg.

Table 9 Summary of the profitability analysis for the conceptual designs of CNT processes

Economic analysis Index	HiPCO process	CoMoCAT process
Total plant costs	\$4.6 million	\$4.4 million
Total product costs	\$186 million	\$124 million
Annual sales revenue	\$450 million	\$450 million
Economic price	\$38/kg	\$25/kg
Net present value (NPV)	\$609 million	\$753 million
Rate of return (ROR)	37.4%	48.2%

Energy consumption, emissions and sustainability

The processes are economically feasible, but they must be move toward sustainability. Both processes operate at high temperature and relatively high pressure. They are energy intensive with significant carbon dioxide emissions, 2,700 kg/h which would increase the concentration of greenhouse gases in the atmosphere.

Sustainable development is the concept that development should meet the needs of the present without compromising of the future to meet its needs (Xu et al. 2005). In order to ensure the sustainability of the proposed production processes, the carbon dioxide emissions from these processes could be utilized as raw materials in other carbon dioxide consuming processes, such as the production of urea, and methanol as described by Xu et al. (2005).

A comparison of these processes can be made using total cost assessment which includes the evaluation of the ''triple bottom line'' or the sum of economic, environmental and sustainable costs. Estimates of the sustainable cost carbon dioxide are of the order of \$50 per ton. The results from this work will be used for evaluations of total cost assessment, inherently safer design and hazard analysis in future research to assess the best design that minimizes the ''triple bottom line''.

Summary

Laboratory-scale carbon nanotube synthesis techniques used either condensation of a carbon vapor or the catalytic action of transition metal particles on carbon vapor. The catalytic chemical vapor deposition processes appeared to be the most promising for an industrial chemical reactor. Two catalytic chemical vapor deposition reactors were selected for the conceptual design of carbon nanotube processes. The reactors use the high-pressure carbon monoxide disproportionation reaction over iron catalytic particle clusters (HiPCO reactor), and the catalytic disproportionation of carbon monoxide or hydrocarbon over a silica supported cobalt–molybdenum catalyst (CoMoCAT reactor). Purification of the carbon nanotube product uses a multi-step approach: oxidation, acid treatment, filtration and drying. The oxidation treatment is used to selectively remove amorphous carbon impurities without affecting the structural integrity of the carbon nanotube product.

The high-pressure carbon monoxide CNT-PFR process used a gas-phase homogeneous reactor where the catalyst was formed from the decomposition of iron

pentacarbonyl (HiPCO reactor). Carbon nanotubes were produced by the disproportionation of carbon monoxide over catalytic iron nanoparticles at 1,323 K and 450 psia. The CO conversion and selectivity to carbon nanotubes was is 20 mol and 90%, respectively. The carbon nanotubes produced contain amorphous carbon and residual iron particles. These impurities were removed in a multi-step purification process, which include oxidation, acid treatment, and filtration. The amorphous carbon and residual iron particles in the nanotube product were selectively oxidized in air to carbon dioxide and iron oxides. The iron oxides formed were subsequently removed by dissolution in concentrated hydrochloric acid solution. The final carbon nanotube product contained 3 mol% residual iron chloride.

The cobalt–molybdenum catalyst CNT-FBR process used a fluidized bed reactor where the carbon nanotubes were formed from carbon monoxide at 1,223 K and 150 psia on the silica-supported Co–Mo bimetallic catalyst particles (CoMoCAT reactor). The carbon monoxide conversion and selectivity to carbon nanotubes was 20 mol and 80%, respectively. The carbon nanotube and amorphous carbon produced were grown and remain attached to the supported catalysts particles. The carbon nanotubes-silica support interaction is broken by treating the reactor product with sodium hydroxide. The carbon nanotubes were subsequently separated from amorphous carbon, silica, and the bulk of the cobalt and molybdenum particles by froth flotation to a purity of 80%. Residual cobalt and molybdenum particles were subsequently removed by dissolution in concentrated hydrochloric acid. The final carbon nanotube product contained; 5 mol% residual cobalt and 1.5 mol% residual molybdenum.

Profitability analysis for the CNT-PFR and CNT-FBR process designs showed that both were economically feasible. For the CNT-PFR process, the net present value, based on a minimum attractive rate of return of 25% and an economic life of 10 years, was $609 million, the rate of return was 37.4% and the economic price was $38 per kg of carbon nanotube. For the CNT-FBR process, the net present value was $753 million, rate of return was 48.2% and the economic price was $25 per kg of carbon nanotube. The economic price for these processes is an order of magnitude less than the prevalent market price of carbon nanotubes and is comparable to the price of carbon fibers.

Acknowledgments This research was supported by the Gulf Coast Hazardous Substance Research Center. This consideration is gratefully acknowledged.

References

Agboola (2005) Development and model formulation of scalable carbon nanotube processes: HiPCO and CoMoCAT process models, M.S. thesis, Louisiana State University, Baton Rouge

Ajayan PM (2000) Carbon nanotubes. Handbook Nanostruct Mat Nanotechnol 5:375–403

Andrews R, Jacques D, Qian D, Rantell T (2002) Multi-wall carbon nanotubes: synthesis and application. Acc Chem Res 35:1008–1017

Bandow S, Rao AM, Williams KA Thess A, Smalley RE, Eklund PC (1997) Purification of single-wall carbon nanotubes by microfiltration. J Phys Chem B 101:8839–8842

Bronikowski MJ, Willis PA, Colbert TD, Smith KA Smalley RE (2001) Gas-phase production of carbon single-walled nanotubes from carbon monoxide via the HiPCO process: a parametric study. J Vacuum Sci Technol A 19(4):1800–1805

Brumby HA, Verhelst MP (2005) Recycling of GTL catalysts, ptqcatalysis. Pet Technol Q Rev p 15

Chemical Engineering (2005) Chemical engineering product cost index. Chem Eng 2005

Chiang IW, Brinson BE, Smalley RE, Margrave JL, Hauge RH (2001a) Purification and characterization of single-wall carbon nanotubes. J Phys Chem B 105:1157–1161

Chiang IW, Brinson BE, Huang AY, Willis PA, Bronikowski MJ, Smalley RE, Margrave JL, Hauge RH (2001b) Purification and characterization of single-wall carbon nanotubes obtained from the gas-phase decomposition of CO (HiPCO). J Phys Chem B 105:8297–8301

Corrias M et al. (2003) Carbon nanotubes produced in a fluidized bed catalytic CVD: first approach of the process. Chem Eng Sci 58:4475–4482

Dateo CE, Gokcen T, Meyyappan M (2002) Modeling of the HiPCO process for carbon nanotube production 1: chemical kinetics. J Nanosci Nanotechnol 2(5):523–534

Davis VA (2005) Carbon nanotechnology laboratory, Chemical Engineering Department, Rice University, Private Communication, January, 2005

Dresselhaus MS, Dresselhaus G, Eklund PC (1996) Science of fullerenes and carbon nanotube. National Academy, Washington

Felder RM, Rousseau RW (2000) Elementary principles of chemical processes. 3rd edn, Wiley, New York

Georgakilas V, Voulgaris D, Vasquez E, Prato M, Guldi DM, Kukovecz A, Kuzmany H (2002) Purification of HiPCO carbon nanotubes via organic functionalization. J Am Chem Soc 124:14318–14319

Guo T, Nikolaev P, Thess A, Colbert DT, Smalley RE (1995) Catalytic growth of single-walled nanotubes by laser vaporization. Chem Phys Lett 243:49–54

Han HJ, Yoo J (2002) Low temperature synthesis of carbon nanotubes by thermal chemical vapor deposition using Co-catalyst. J Korean Phys Soc 39:S116–S119

Harutyunyan AR, Pradhan BK, Chang J, Chen G, Eklund PC (2002) Purification of single-wall carbon nanotubes by selective microwave heating of catalyst particles. J Phys Chem B 106:8671–8675

Hernadi K, Fonseca A, Nagy JB, Bernaerts D, Riga J, Lucas A (1996) Catalytic synthesis and purification of carbon nanotubes. Sync Metals 77:31–34

Hou PX, Bai S, Yang QH, Liu C, Cheng HM (2002) Multi-step purification of carbon nanotubes. Carbon 40:81–85

Iijima S, Ajayan PM, Ichiashi T (1992) Growth model for carbon nanotubes. Phys Rev Lett 69(21):3100–3103

Journet C, Maser WK, Bernier P, Loiseau A, Lamy de la Chapelle M, Lefrant S, Denlard P, Lee R, Fischer JE (1997) Large-scale production of single-walled carbon nanotubes by the electric-arc technique. Nature 388:756–758

Lee SJ, Baik HK, Yoo J, Han JH (2002) Large scale synthesis of carbon nanotubes by plasma rotating arc discharge technique. Diamond Relat Mat 11:914–917

Li M, Hu Z, Wang X, Wu Q, Chen Y, Tian Y (2004) Low temperature synthesis of carbon nanotubes using corona discharge plasma at atmospheric pressure. Diamond Relat Mat 13:111–115

Liu X, Huang B, Coville NJ (2002) The influence of synthesis parameters on the production of multi-walled carbon nanotubes by the ferrocene catalyzed pyrolysis of toluene. Fullerenes Nanotubes Nanostruct 10(4):339–352

Lyu SC, Liu BC, Lee SH, Park CY, Kang HK, Yang CW, Lee CJ (2004) Large-scale synthesis of high-quality single-walled carbon nanotubes by catalytic decomposition of ethylene. J Phys Chem B 108:1613–1616

Mauron Ph, Emmenegger Ch, Sudan P, Wenger P, Rentsch S, Zuttel A (2003) Fluidized-bed CVD synthesis of carbon nanotubes on Fe_2O_3/MgO. Diamond Relat Mat 12:780–785

McBride BJ, Zehe M, Gordon S (2002) NASA Glenn coefficients for calculating thermodynamic properties, NASA/TP-2002, 211556

Meyyappan M (2004) Growth: CVD and PECVD. Carbon nanotubes: science and applications. CRC Press, Boca Raton, pp 99–116

Meyyappan W, Srivasta D (2003) Handbook of nanoscience. Eng Technol 18:18-1–18-26

Moravsky AP, Wexler EU, Loutfy RO (2005) Growth of carbon nanotubes by arc discharge and laser ablation. Carbon nanotubes: science and applications 65–98 Nikolaev, 2004

Nikolaev P (2004) Gas-phase production of single wall carbon nanotubes from carbon monoxide: A review of the HiPCO process. J Nanosci Technol 4(4):307–316

Niyogi S, Hu H, Hamon MA, Bhowmik P, Zhao B, Rozenzhak SM, Chen J, Itkis ME, Meier M S, Haddon RC (2001) Chromatographic purification of soluble single-walled carbon nanotubes (s-SWNTs). J Am Chem Soc 123:733–734

Park YS, Choi YC, Kim KS, Chung DC, Bae DJ, An KH, Lim SC, Zhu XY, Lee YH (2001) High yield purification of multi-walled carbon nanotubes by selective oxidation during thermal annealing. Carbon 39:655–661

Perez-Cabero M, Rodriguez-Ramos I, Guerrero-Ruiz A (2003) Characterization of carbon nanotubes and carbon nanofibers prepared by catalytic decomposition of acetylene in a fluidized bed reactor. J Catal 215:305–316

Pisan C, Chavadej S, Kitiyana B, Scamehorn JF, Resasco DE (2004) Separation of single-wall carbon nanotubes from silica by froth flotation technique. AIChE Annual Meeting, Indianapolis

Resasco DE, Alvarez WE, Pompeo F, Balzano L, Herrera JE, Kitiyanan B, Borgna A (2001) A scalable process for production of single-walled carbon nanotubes by catalytic disproportionation of CO on a solid catalyst. J Nanopart Res 00:1–6

Scott CD, Povitsky A, Dateo C, Willis PA, Smalley RE (2003) Iron catalyst chemistry in modeling a high-pressure carbon monoxide reactor. J Nanosci Nanotechnol 3:63–73

Shelimov KB, Esenaliev RO, Rinzler AG, Huffman CB, Smalley RE (1998) Purification of single-wall carbon nanotubes by ultrasonically assisted filtration. Chem Phys Lett 282:429–434

Terrones M (2003) Science and technology of the twenty- first century: synthesis, properties and applications of carbon nanotubes. Ann Rev Mat Res 33:419–509

Thien-Nga L, Hernadi K, Ljubovic E, Garaj S, Forro L (2002) Mechanical purification of single-walled carbon nanotube bundles from catalytic particles. Nano Lett 2(12):1349–1352

Turton R, Bailie RC, Whiting WB, Shaeiwitz JA (1998) Analysis, synthesis and design of chemical processes. 2nd edn, Prentice-Hall, New York

Xu A, Pike RW, Indala S, Knopf FC, Yaws CL, Hopper JR (2005) Development and integration of new processes consuming carbon dioxide in multi-plant chemical complexes. Clean Technol Environ Policy, vol 7(2) pp 97–115